Journal of Communications Technology and Electronics, Vol. 50, No. 2, 2005, pp. 227–233. Translated from Radiotekhnika i Elektronika, Vol. 50, No. 2, 2005, pp. 245–251.

RADIO PHENOMENA IN SOLIDS AND PLASMA

Numerical Simulation of Electrically Conducting Liquid Flows in an External Magnetic Field

T. G. Elizarova, I. S. Kalachinskaya, Yu. V. Sheretov, and I. A. Shirokov

Received June 25, 2004

Abstract—In terms of the quasi-hydrodynamic approach, a new algorithm for numerical analysis of convective flows of semiconductor melts in the presence of a uniform external magnetic field is proposed. The Marangoni convection problem is solved for square and cylindrical caverns.

INTRODUCTION

It is known that a convective flow that arises in a melt under the action of gravitational or thermocapillary forces is damped by applying an external magnetic field to the system. The possibility of employing this effect for improving the properties of crystals grown using the floating-zone method is widely studied nowadays by means of both full-scale experiments [1, 2] and simulations [3, 4]. In the modern state of the art, simulation of the magnetic-field interaction with an electrically conducting liquid is a challenge in terms of both theory and computations.

In this study, we elaborate in more detail the quasi-hydrodynamic (QHD) model proposed in [5] for the description of quasi-neutral conducting liquid flows in an external magnetic field. A simplified variant is constructed with an orientation to planar and axisymmetric flows of semiconductor melts. Results of calculations are presented to demonstrate the workability of the numerical algorithm applied.

Since 1997, the unconventional approach to simulation of gas flows based on QHD equations was repeatedly reported during scientific seminars held at the Faculty of Physics, Moscow State University, and chaired by A.G. Sveshnikov, whose constant support and encouragement largely promoted the development of this new line of research.

1. A MATHEMATICAL BACKGROUND

For the quantities characterizing convective flows of a quasi-neutral conducting liquid, we use the following denotations: $\rho = \text{const} > 0$ is the mean density; $\vec{u} = \vec{u}(\vec{x}, t)$ is the hydrodynamic velocity; $p = p(\vec{x}, t)$ is the pressure measured relative to the hydrostatic value; $T = T(\vec{x}, t)$ is the deviation of temperature from the mean value $T_0 = \text{const} > 0$; and $\vec{H} = \vec{H}(\vec{x}, t)$ and $\vec{E} = \vec{E}(\vec{x}, t)$ are the strengths of the magnetic and electric fields, respectively. As the basic mathematical model, we employ the quasi-magnetohydrodynamic (QMHD) system within the Oberbeck–Boussinesq approximation, as proposed in [5]. This system can be represented in the form

$$\operatorname{div}\vec{u} = \operatorname{div}\vec{w}, \tag{1}$$

$$\frac{\partial \vec{u}}{\partial t} + \operatorname{div}(\vec{u}\otimes\vec{u}) + \frac{1}{\rho}\vec{\nabla}p = -\beta\vec{g}T + \frac{1}{\rho}\operatorname{div}\Pi_{\text{NS}} + \operatorname{div}[(\vec{w}\otimes\vec{u}) + (\vec{u}\otimes\vec{w})] + \frac{1}{\rho c}(\vec{j}_e\times\vec{H}), \tag{2}$$

$$\frac{\partial T}{\partial t} + \operatorname{div}(\vec{u}T) = \operatorname{div}(\vec{w}T) + \chi\Delta T, \tag{3}$$

$$\operatorname{curl}\vec{E} = -\frac{1}{c}\frac{\partial \vec{H}}{\partial t}, \quad \operatorname{div}\vec{H} = 0, \quad \vec{j}_e = \frac{c}{4\pi}\operatorname{curl}\vec{H}. \tag{4}$$

Here,

$$\Pi_{\text{NS}} = \eta[(\vec{\nabla}\otimes\vec{u}) + (\vec{\nabla}\otimes\vec{u})^T] \tag{5}$$

is the Navier–Stokes tensor of viscous stress and $\otimes$ indicates the scalar product. The electric current density can be calculated from

$$\vec{j}_e = \sigma\left(\vec{E} + \frac{1}{c}((\vec{u}-\vec{w})\times\vec{H})\right), \tag{6}$$

where

$$\vec{w} = \tau\left[(\vec{u}\cdot\vec{\nabla})\vec{u} + \frac{1}{\rho}\vec{\nabla}p + \beta\vec{g}T - \frac{1}{\rho c}(\vec{j}_e\times\vec{H})\right]. \tag{7}$$

In Eqs. (1)–(7), temperature expansion coefficient for the liquid β, dynamic viscosity $\eta = \rho\nu$, thermal diffusivity χ, and electrical conductivity σ are given positive constants. Vector $\vec{g}$ is the free-fall acceleration, and c is the velocity of light in free space. Relaxation parameter τ, having the dimension of time, is related to kinematic

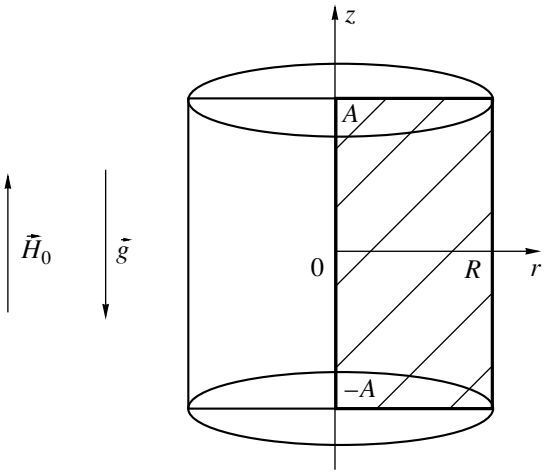

Fig. 1. Schematic of the calculation region (hatched) in the problem for a cylindrical cavern.

viscosity coefficient ν and velocity of sound in the absence of electromagnetic field c_{sn} by the expression $\tau = \nu/c_{sn}^2$. Equations (1)–(7) are written with the use of the standard notation of tensor analysis.

2. STATEMENT OF THE PROBLEM

Let us consider axisymmetric flows of a semiconductor melt in a cylindrical cavity with rigid walls. Let us assume that $\Omega = \{(r, z) : 0 < r < R, -A < z < A\}$ is a calculation area, external magnetic field $\vec{H}_0$ is uniform and directed along the symmetry axis of the cylinder, and vector $\vec{g}$ is directed in the opposite direction $\vec{H}_0$ (Fig. 1).

The noninductive approximation of system of equations (1)–(7) in cylindrical coordinates (r, z) appears in the form

$$\frac{1}{r}\frac{\partial}{\partial r}\left(r\frac{\partial p}{\partial r}\right) + \frac{\partial^2 p}{\partial z^2} = \frac{1}{\tau}\left[\frac{1}{r}\frac{\partial (ru_r)}{\partial r} + \frac{\partial u_z}{\partial z}\right]$$

$$-\frac{1}{r}\frac{\partial}{\partial r}\left[r\left(u_r\frac{\partial u_r}{\partial r} + u_z\frac{\partial u_r}{\partial z} + \mathrm{Ha}^2 u_r\right)\right] \qquad (8)$$

$$-\frac{\partial}{\partial z}\left(u_r\frac{\partial u_z}{\partial r} + u_z\frac{\partial u_z}{\partial z} - \mathrm{Gr}T\right),$$

$$\frac{\partial u_r}{\partial t} + \frac{1}{r}\frac{\partial (ru_r^2)}{\partial r} + \frac{\partial (u_z u_r)}{\partial z} + \frac{\partial p}{\partial r}$$

$$= \frac{1}{r}\frac{\partial (r\Pi_{rr}^{\mathrm{NS}})}{\partial r} + \frac{\partial \Pi_{zr}^{\mathrm{NS}}}{\partial z} - \frac{\Pi_{\varphi\varphi}^{\mathrm{NS}}}{r} \qquad (9)$$

$$+\frac{2}{r}\frac{\partial (ru_r w_r)}{\partial r} + \frac{\partial (u_r w_z)}{\partial z} + \frac{\partial (u_z w_r)}{\partial z} - \mathrm{Ha}^2(u_r - w_r),$$

$$\frac{\partial u_z}{\partial t} + \frac{1}{r}\frac{\partial (ru_r u_z)}{\partial r} + \frac{\partial (u_z^2)}{\partial z} + \frac{\partial p}{\partial z}$$

$$= \frac{1}{r}\frac{\partial (r\Pi_{rz}^{\mathrm{NS}})}{\partial r} + \frac{\partial \Pi_{zz}^{\mathrm{NS}}}{\partial z} + \frac{1}{r}\frac{\partial (ru_z w_r)}{\partial r} \qquad (10)$$

$$+\frac{1}{r}\frac{\partial (ru_r w_z)}{\partial r} + 2\frac{\partial (u_z w_z)}{\partial z} - \mathrm{Gr}T,$$

$$\frac{\partial T}{\partial t} + \frac{1}{r}\frac{\partial (ru_r T)}{\partial r} + \frac{\partial (u_z T)}{\partial z}$$

$$= \frac{1}{r}\frac{\partial (rw_r T)}{\partial r} + \frac{\partial (w_z T)}{\partial z} + \frac{1}{\mathrm{Pr}}\left[\frac{1}{r}\frac{\partial}{\partial r}\left(r\frac{\partial T}{\partial r}\right) + \frac{\partial^2 T}{\partial z^2}\right]. \qquad (11)$$

Here,

$$w_r = \tau\left(u_r\frac{\partial u_r}{\partial r} + u_z\frac{\partial u_r}{\partial z} + \frac{\partial p}{\partial r} + \mathrm{Ha}^2 u_r\right), \qquad (12)$$

$$w_z = \tau\left(u_r\frac{\partial u_z}{\partial r} + u_z\frac{\partial u_z}{\partial z} + \frac{\partial p}{\partial z} - \mathrm{Gr}T\right). \qquad (13)$$

The components of Navier–Stokes viscous stress tensor Π^{NS} can be calculated by formulas

$$\Pi_{rr}^{\mathrm{NS}} = 2\frac{\partial u_r}{\partial r}, \quad \Pi_{zr}^{\mathrm{NS}} = \Pi_{rz}^{\mathrm{NS}} = \left(\frac{\partial u_r}{\partial z} + \frac{\partial u_z}{\partial r}\right),$$

$$\Pi_{\varphi\varphi}^{\mathrm{NS}} = 2\frac{u_r}{r}, \quad \Pi_{zz}^{\mathrm{NS}} = 2\frac{\partial u_z}{\partial z}.$$

System of equations (8)–(13) is represented in a dimensionless form. It can be derived from Eqs. (1)–(7) under the following simplifying assumptions: (i) the induced currents are small and the electric-field effect is negligible and (ii) the magnetic field in the liquid that fills the cavity deviates from $\vec{H}_0$ only slightly.

Mass conservation law (1) is written in the form of the Poisson equation for pressure (8).

It is convenient to measure r, z, t, u_r, u_z, w_r, w_z, p, and T in terms of R, R, R^2/ν, ν/R, ν/R, ν/R, ν/R, $\rho(\nu/R)^2$, and Θ, respectively, where Θ is the temperature at the point (1, 0). Dimensionless value τ is calculated by the formula

$$\tau = \frac{1}{\mathrm{Re}_{sn}^2}. \qquad (14)$$

The Grashof (Gr), Hartmann (Ha), Prandtl (Pr), and Reynolds (Re_{sn}) numbers are determined from the expressions

$$\mathrm{Gr} = \frac{g\beta\Theta R^3}{\nu^2},\ \mathrm{Ha} = \frac{RH_0}{c}\sqrt{\frac{\sigma}{\eta}},\ \mathrm{Pr} = \frac{\nu}{\chi},\ \mathrm{Re}_{sn} = \frac{c_{sn}R}{\nu}.$$

Let the cylinder height be $2A = 2R = 2$. The filling liquid is assumed to stick to the cylinder's upper and lower faces. The initial conditions are presented as

$$(u_r)|_{t=0} = (u_z)|_{t=0} = 0, \quad T|_{t=0} = 1 - |z|. \quad (15)$$

The external surface is subjected to the action of surface-tension forces, which depend on the temperature regime chosen.

Let us represent the boundary conditions in the following forms:

(i) on the symmetry axis ($r = 0, -1 < z < 1$);

$$u_r = 0, \quad \frac{\partial u_z}{\partial r} = 0, \quad \frac{\partial p}{\partial r} = 0, \quad \frac{\partial T}{\partial r} = 0; \quad (16)$$

(ii) on the lateral wall ($r = 1, -1 < z < 1$);

$$u_r = 0, \quad \frac{\partial u_z}{\partial r} = -\frac{\mathrm{Ma}}{\mathrm{Pr}}\frac{\partial T}{\partial z}, \quad \frac{\partial p}{\partial r} = 0, \quad T = 1 - |z|; \quad (17)$$

(iii) on the lower ($0 < r < 1, z = -1$) and the upper ($0 < r < 1, z = 1$) ends:

$$u_r = u_z = 0, \quad \frac{\partial p}{\partial z} = \mathrm{Gr}T, \quad T = 0. \quad (18)$$

Here,

$$\mathrm{Ma} = -\frac{\Theta R}{\eta\chi}\frac{\partial\sigma_T}{\partial T}$$

is the Maragoni number and σ_T is the surface-tension coefficient. In order to exclude ambiguity in defining the pressure, we use the normalization $p(0, 0) = 0$. For the statement of the problem and the system of QMHD equations for the case of a planar flow, see [6].

3. THE NUMERICAL PROCEDURE AND EXAMPLES OF THE CALCULATION

The initial-boundary-value problem (8)–(18) is solved according to the explicit finite-difference scheme of the second order described in [6, 7]. Stationary flows are found with the use of the iteration method for $t \longrightarrow \infty$. Iterations are performed until

$$\frac{1}{N_r N_z}\max\sum_{i,j}\left|(u^{\mathrm{up}})_{ij} - u_{ij}\right| < \varepsilon,$$

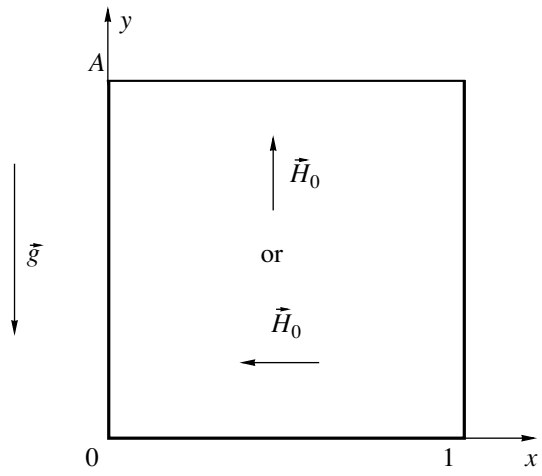

Fig. 2. Schematic of the calculation region (hatched) in the problem for a square cavern.

where $(u^{\mathrm{up}})_{ij}$ are the components of the velocity at the upper time layer at points (i, j); ε is a given accuracy; and N_r and N_z are the numbers of points of the difference mesh in the r and z directions, respectively. At each time step, Poisson equation (8) is solved using the iteration method, which was adapted to a cluster-based multiprocessor computer system [8].

In order to ensure the stability of solution, the value of τ (see (14)) is calculated as

$$\tau = \frac{1}{\mathrm{Re}_{sn}^2} + \tau_0,$$

where τ_0 is the regularizing parameter to be matched during the calculation. For the flows studied, the number Re_{sn} is fairly high. When $L = 1$ cm, $\nu \sim 0.01$ cm^2/s, and $c_{sn} \sim 10^5$ cm/s, the corresponding Re_{sn} is of on the order of 10^7. Therefore, one can consider $\tau = \tau_0$.

Numerical calculations were performed to verify the workability of the algorithm used to solve the QMHD equations, and the convergence of the difference solution under spatial-mesh condensation was investigated. We also studied the influence of the magnetic field on the structure and intensity of convective motion in the melt by analyzing the thermocapillary convection of a semiconductor melt in a cylindrical (see Fig. 1) and a square-plane cavern (Fig. 2) in the absence of gravity (Gr = 0). In this case, a convective flow is induced by the surface tension. The calculation was carried out for the following values of dimensionless parameters: $A = 1$, Ma = 1000, Pr = 0.018, and Ha = 0, 50, 100. In all cases, the time step was $\Delta t = 10^{-7}$.

In the calculation for the cylindrical cavern (Fig. 1), the dimensionless parameter was $\tau = 2 \times 10^{-7}$. The flow was considered steady when $\varepsilon = 10^{-4}$. A uniform mesh

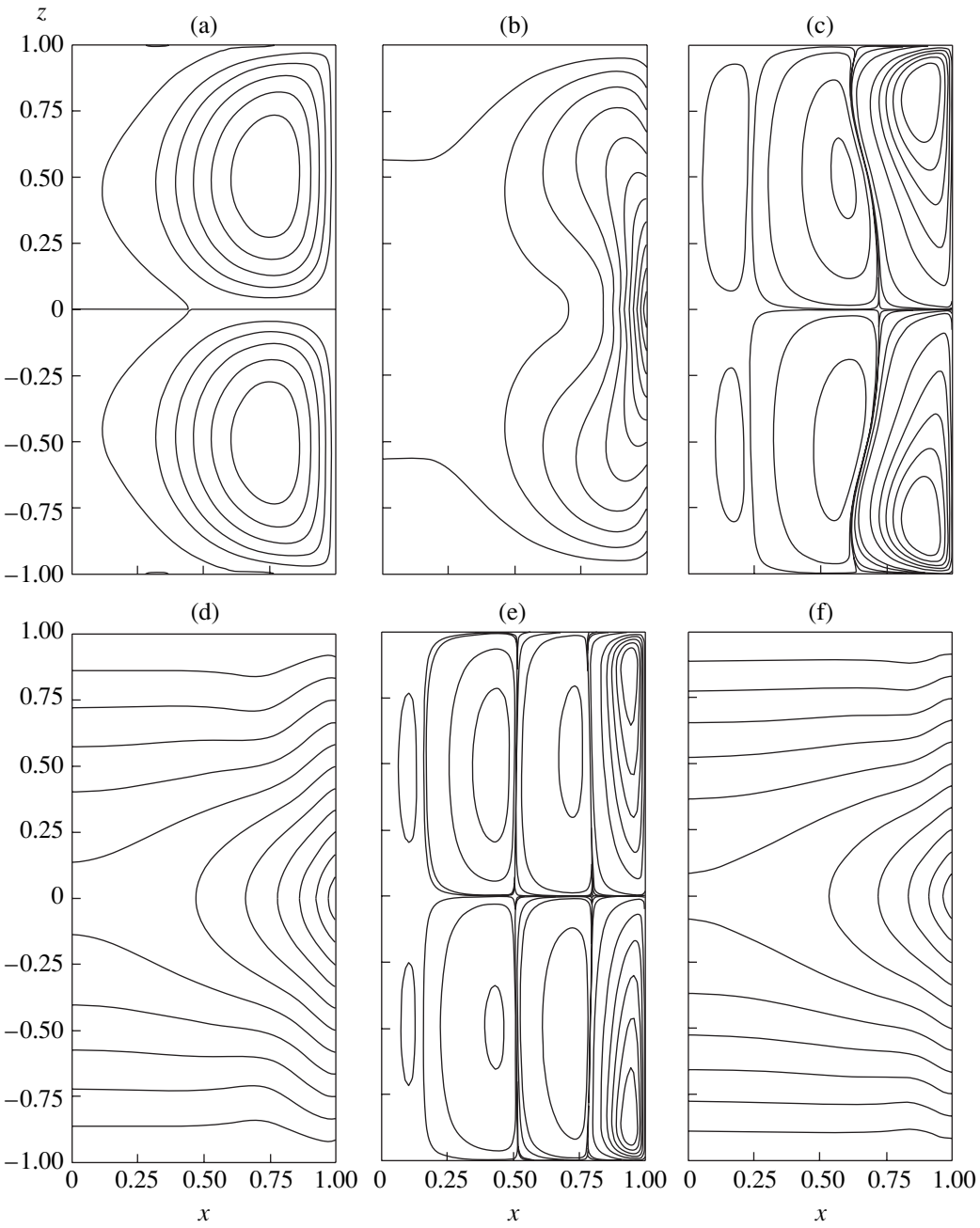

Fig. 3. Contour lines of the (a, c, e) stream function and (b, d, f) temperature in a cylindrical cavern for Ha = (a, b) 0, (c, d) 50, and (e, f) 100.

with square cells was used. The calculation was carried out by means of an MVS-1000M multiprocessor cluster computer system complying with the MPI standard.

It was found that the number of time steps to the steady state appreciably reduces with an increase in the Hartmann number (see Table 1). This fact is explained by a decrease in the convection velocities in the presence of the magnetic field. As the intensity of the magnetic field grows, the flow becomes multilayered with the main vortex shifted towards the free surface of the melt.

Figure 3 show the contour lines of temperature and the stream function. It is seen that the isotherms and streamlines are equidistant in the vicinity of the main vortex. Stream function ψ is calculated from the expressions

$$u_r - w_r = -\frac{1}{r}\frac{\partial\psi}{\partial z}, \quad u_z - w_z = \frac{1}{r}\frac{\partial\psi}{\partial r}$$

with the normalization $\psi = 0$ at the boundary. The flow obtained is symmetrical about the plane $z = 0$, which is

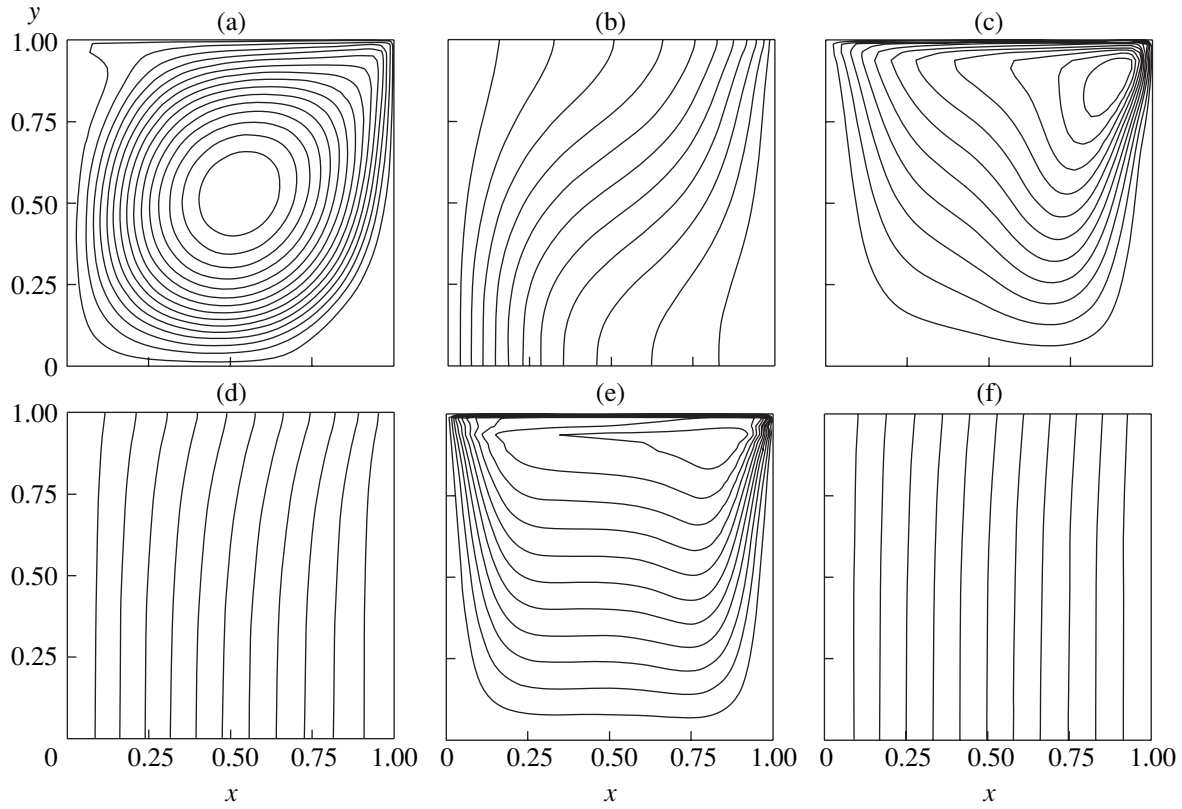

Fig. 4. Contour lines of the (a, c, e) stream function and (b, d, f) temperature in a square cavern in the vertical magnetic field for Ha = (a, b) 0, (c, d) 50, and (e, f) 100.

due to the prescribed symmetric distribution of temperature over the lateral wall and the absence of gravity (Gr = 0). The results for Ha = 100 (see Table 1) bear evidence of the convergence of the applied numerical procedure.

During simulation of the flow in a square cavity (Fig. 2) it was assumed that the adiabaticity of the cavity's upper and lower faces yielded the boundary conditions for temperature. We set $T = 1$ and $T = 0$ on the left and the right walls, respectively. Dimensionless parameter τ was set equal to 2×10^{-5}. The flow was considered steady when accuracy $\varepsilon = 10^{-3}$ was attained. The series of uniform spatial meshes with the numbers of nodes 22×22, 42×42, and 82×82 was used. We considered two cases related to vertically and horizontally oriented magnetic fields. The results obtained in the steady mode are presented in Figs. 4 and 5 and in Table 2. Arrows indicate the directions of the magnetic field.

In the case of the vertical magnetic field, Fig. 4 displays the isotherms and the isolines of the stream function for various Hartmann numbers, as obtained with the 42×42 mesh. Both the isotherms and isolines of the stream function are equidistant. The stream function is defined by the expressions

$$u_x - w_x = \frac{\partial \psi}{\partial y}, \quad u_y - w_y = -\frac{\partial \psi}{\partial x}.$$

At the boundaries of the calculation area, stream function ψ vanishes. The minimum values of ψ are listed in Table 2. As the magnetic field increases, the convective flow in the cavern slows down and the vortex shifts to the right and upwards, thus, concentrating near the free surface of the melt. At Ha = 100, the distortion of the isotherms caused by the melt flow is very small.

The isotherms and streamlines are presented in Fig. 5 in the case of the horizontal magnetic field. It is seen that the streamlines in the upper part of the maps and the isotherms are equidistant. The maximum absolute values of the stream function appear to be higher

Table 1. Calculation parameters for a cylindrical cavern

Ha	Mesh size $N_r \times N_z$	The number of steps to the steady state	Stream function minimum ψ_{min}
0	82×162	569477	–249.6
50	82×162	84326	–52.2
100	82×162	45400	–37.1
100	162×322	45574	–37.0

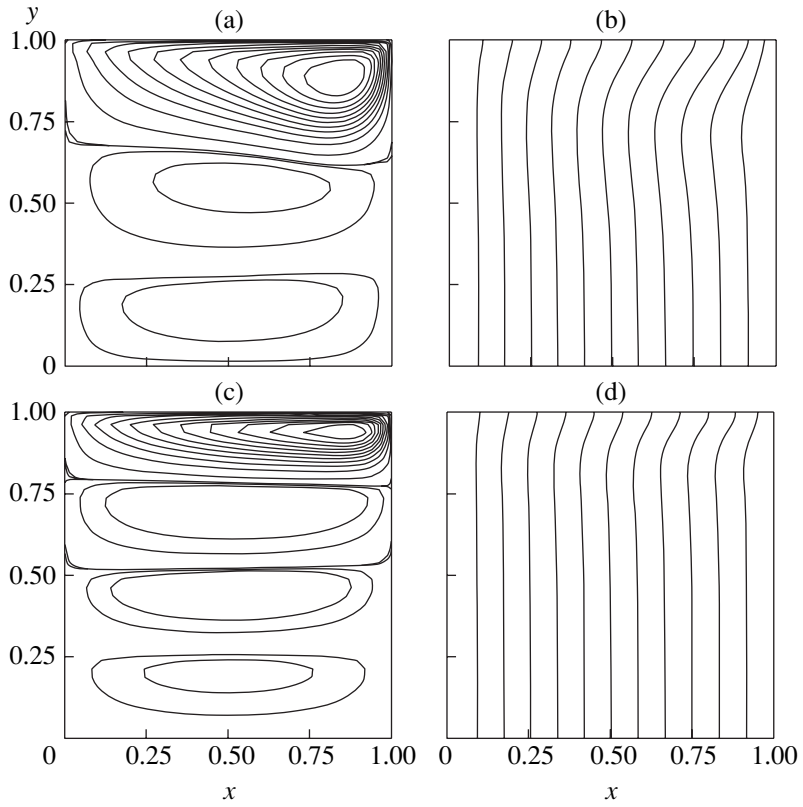

Fig. 5. Contour lines of the (a, c) stream function and (b, d) temperature in a square cavern in the horizontal magnetic field for Ha = (a, b) 50 and (c, d) 100.

than the corresponding values obtained for the vertical field. The main vortex shifts noticeably towards the upper surface, and the flow as a whole becomes multilayered. At Ha = 50 and 100, three and four vortices, respectively, are observed. Similar dependences were obtained in the calculations of flow in the cylindrical geometry (see Fig. 3).

In study [4], a similar problem was solved using the finite-difference algorithm based on the Navier–Stokes equations. An implicit finite-difference scheme of the third-order spatial accuracy was constructed in natural variables. In order to verify the method proposed, we calculated the melt's stream field in the statement presented in [4]. With the 42×42 mesh, the minimum value of the stream function at the center of the main vortex was found to be $\psi_{min} = -43.5$ at Ha = 50. The result obtained in [4] was $\psi_{min} = -44.2$. The general flow structure in both cases was almost identical. This comparison illustrates the high accuracy of the approach applied.

Table 2. Calculation parameters for a square cavern

Ha	Mesh size $N_x \times N_y$	The number of steps to the steady state	Stream function minimum ψ_{min}
50↑	22×22	437210	–23.83
0	42×42	1500000	–134.3
50 ↑	42×42	440130	–22.18
100 ↑	42×42	353705	–5.224
50 ←	42×42	441100	–47.785
100 ←	42×42	375754	–41.124
50 ↑	82×82	439553	–21.88

CONCLUSIONS

An original mathematical model of flows in a quasi-neutral compressible electrically conducting liquid, referred to as a QMHD system, has been considered. Based on this model, a simplified model of a QMHD system in the noninductive Oberbeck–Boussinesq approximation has been constructed and applied to numerically simulate semiconductor-melt flows in an external magnetostatic field. The numerical algorithm described presents a time-explicit uniform finite-difference scheme with special regularizing parameters, which provide for the high accuracy and stability of numerical solution.

A series of simulations has been carried out to calculate thermocapillary flows of a semiconductor melt in cylindrical and square caverns at various strengths and orientations of the external magnetic field. It has been established that the magnetic field slows down the convective liquid motion and drives it towards the free surface. In the case when the magnetic-field strength is parallel to the free surface, the flow becomes multilayered.

Numerical data have been compared to the results obtained using the classical magnetohydrodynamic system in the noninductive approximation. This has shown that the model proposed and the numerical method of its integration are highly efficient for calculating the conducting liquid flows with an acceptable accuracy, even at comparatively coarse spatial meshes.

REFERENCES

1. P. Dold, A. Croll, and K. W. Benz, J. Cryst. Growth **183**, 545 (1998).
2. A. Croll, F. R. Szofran, P. Dold, *et al.*, J. Cryst. Growth **183**, 554 (1998).
3. Th. Kaiser and K. W. Benz, J. Cryst. Growth **183**, 564 (1998).
4. A. I. Feonychev and G. A. Dolgikh, Kosm. Issled. **39**, 390 (2001).
5. Yu. V. Sheretov, *Mathematical Modeling of Liquid and Gas Flows on the Basis of Quasi-Hydrodynamic and Quasi-Gasdynamic Equations* (Tversk. Gos. Univ., Tver', 2000) [in Russian].
6. T. G. Elizarova, A. V. Zherikov, I. S. Kalachinskaya, and Yu. V. Sheretov, Prikl. Mat. Inform. (Tr. Fak. VMK Mosk. Gos. Univ.), No. 13, 63 (2003).
7. T. G. Elizarova, I. S. Kalachinskaya, A. V. Klyuchnikova, and Yu. V. Sheretov, Zh. Vychisl. Mat. Mat. Fiz. **38**, 1732 (1998) [Comput. Math. Math. Phys. **38**, 1662 (1998)].
8. I. A. Shirokov, Differentsial'nye Uravneniya **39**, 993 (2003).